Turbulent Convective Heat Transfer and Pressure Drop of Dilute CuO (Copper Oxide) - Water Nanofluid Inside a Circular Tube

Eldwin DJAJADIWINATA [1,*], Hany A. AL-ANSARY [1], Khalid AL-DAKKAN [2], Abdulaziz BAGABAS [2], Abdulaziz AL-JARIWI [2], Mohamed F. ZEDAN [1]

* Corresponding author: Tel.: +966-530823159; Email: eldwin_dj@yahoo.com
1: Department of Mechanical Engineering, College of Engineering, King Saud University, Riyadh, Kingdom of Saudi Arabia
2: National Nanotechnology Center (NNC), King Abdulaziz City for Science and Technology, Riyadh, Kingdom of Saudi Arabia

Abstract Turbulent forced convective heat transfer and pressure drop of 0.01 vol.% CuO-water nanofluid was assessed experimentally. The nanofluids were made flow into a heated horizontal tube under uniform constant heat flux within Reynolds number range of 11,500 to 32,000. The first objective is to know how close traditional correlation/formula for, both, heat transfer and pressure drop can predict nanofluid's heat transfer and pressure drop. The second is to know how nanofluid's convective heat transfer and pressure drop are compared to those of its base fluid; in this case water. The results showed that the abovementioned characteristics of the nanofluid can be predicted by the traditional correlation available. It is also found that the nanofluid's Nusselt number and friction factor, which represent the heat transfer rate and pressure drop, respectively, are close to those of water. Hence, there is no anomaly due to the dispersed nanoparticles within the water.

Keywords: Nanofluid, Copper oxide (CuO), Heat Transfer, Pressure Drop

1. Introduction

In the past 20 years many researchers have been studying the properties of newly emerging fluids which are called nanofluids and are expected to be the next generation of heat transfer fluid due to its better thermal performance compared to that of traditional heat transfer fluid. A nanofluid can be defined as a fluid in which solid particles with sizes below 100 nm are suspended stably and dispersed uniformly. The base fluid used is usually a traditional heat transfer fluid, e.g., water, oil, and ethylene glycol.

A lot of researchers observed the phenomenon of higher thermal conductivity of various nanofluids compared to that of the base fluids. However, there is a main difference between the results, i.e., some results showed that the increase of thermal conductivity of nanofluids is an anomaly that cannot be predicted by the existing conventional equation (Eastman et al. 2001, Murshed et al. 2005) while some others showed that the increase is not an anomaly and can be predicted by using the existing equation (Zhang et al. 2006, Beck et al. 2007).

Regarding the convection heat transfer, Xuan and Li (2003) reported that in turbulent forced convection, the heat transfer coefficient of Cu-water nanofluids flowing inside a uniformly heated tube remarkably increased. The heat transfer coefficient increased by around 39% for 2 vol.% nanoparticle concentration compared to that of water. Furthermore, it was observed that the increase of nanoparticle concentration would also increase the heat transfer coefficient. Interestingly, the experimental results showed that there is no significant increase in pressure drop compared to that of water. Thus, it is no need to be worried about the drawback of pumping power increase.

Maiga et al. (2004) investigated, numerically, laminar and turbulent forced convection of water-γAl_2O_3 and ethylene glycol-γAl_2O_3 nanofluids inside a uniformly heated circular tube. It was found that heat transfer at the tube wall was enhanced for both laminar and turbulent flow compared to that of the base fluids. The enhancement increased with the increase of particle loading. However, this also resulted in the increase of wall shear stress which causes the undesirable increase of pumping power which contradicts the conclusion of Xuan and Li (2003).

Experiments conducted by Heris et al. (2007) showed that the increase of laminar flow convection coefficient of Al_2O_3/water nanofluids under constant wall temperature is much higher than that predicted by single phase heat transfer correlation used in conjunction with the nanofluids' properties. It was also concluded that the heat transfer enhancement of nanofluids is not merely due to the thermal conductivity increase of nanofluids which means other factors may contribute to this phenomenon. The volume concentrations used in this experiment were 0.2%, 0.5%, 1.0%, 1.5%, 2.0%, and 2.5%.

Williams and Buongiorno (2007 and 2008) conducted experiments to investigate heat transfer and pressure loss behavior of alumina (Al_2O_3)/water and zirconia (ZrO_2)/water nanofluids tested in fully developed turbulent flow. The results showed that there was no anomaly in the heat transfer enhancement of the specified nanofluids under the test conditions. It was confirmed that the convective heat transfer and pressure loss behavior can be predicted by means of the conventional correlations and models in conjunction with the use of effective nanofluids' properties for calculating the dimensionless numbers.

Despite the contradictions of some experimental results on forced convective heat transfer inside a tube, the majority of researchers found that nanofluids have better heat transfer performance compared to that of the base fluids, either it can be predicted or not by the conventional correlations. Thus, there is still hope to use nanofluids as a new heat transfer fluid as long as the ratio of heat transfer coefficient to the pumping power of nanofluids is greater than that of the base fluids. Therefore, in order to contribute in searching nanofluids that give good trade-off between increase in heat transfer coefficient and increase in pressure drop, this research experimentally observes the convection heat transfer and pressure drop which occur in a dilute CuO (copper oxide)-water nanofluids.

2. Experimental Setup

To test the heat transfer and pressure drop behavior of nanofluid, a loop, within which the nanofluid flowed, was constructed. It consisted of smooth tube, made of stainless steel (SS316) which outer diameter and thickness were 0.5 in (0.0127 m) and 0.065 in (0.00165 m), respectively. In Fig. 1, it can be seen that in this loop there were two test sections made of the aforementioned tube, namely, (1) heated test-section and (2) isothermal test-section. The former was used to observe, both, heat transfer and pressure drop behavior of the flowing nanofluid, while the latter focused on pressure drop. Pressure drop was measured on both test sections in order to observe the effect of heating of the flowing nanofluid on the pressure drop. The lengths of the test-sections were 3.04 m and 3.00 m for the heated test-section and isothermal test-section, respectively.

The heated test-section was heated by the principle of Ohmic heating by connecting it to a 10 kW DC power supply. The power supply used was GENESYS 10 kW (20 V and 500 A), TDK-Lambda Americas Inc. It has accuracy of 0.5% of its rated (maximum designated) output. SS-8-DE-6 Swagelok dielectric fitting was connected somewhere on the loop as electric breaker in order to confine the electric current flowing only in the heated test-section.

The thermal insulation used on the heated test-section was rigid melamine foam for pipe and tube, 93495K11 McMaster-CARR, with 1 in. (25.4 mm) thickness. The isothermal test-section was also thermally insulated with elastomeric tape to maintain constant temperature of the liquid flowing inside it and to avoid condensation.

For temperature measurements, 14 T-type thermocouples (TJC36-CPSS-032U-12, OMEGA) were attached for every 0.203 m along the top-outer-surface of the heated test-section starting at 0.203 m from the beginning of test-section. Moreover, three T-type thermocouples (TJC36-CPIN-062U-12, OMEGA) were submerged to measure bulk temperature of the nanofluid at three locations, i.e., (1) inlet of the heated test-section, (2) outlet of the heated test-section, and (3) inlet of the isothermal test-section. These thermocouples, as stated by the manufacturer, have accuracy of 0.5 ^{o}C. The test-fluid was pumped by 1 HP stainless steel STA-RITE pump (certified to be equivalent to 1 HP SS1SX1-1 Berkeley pump).

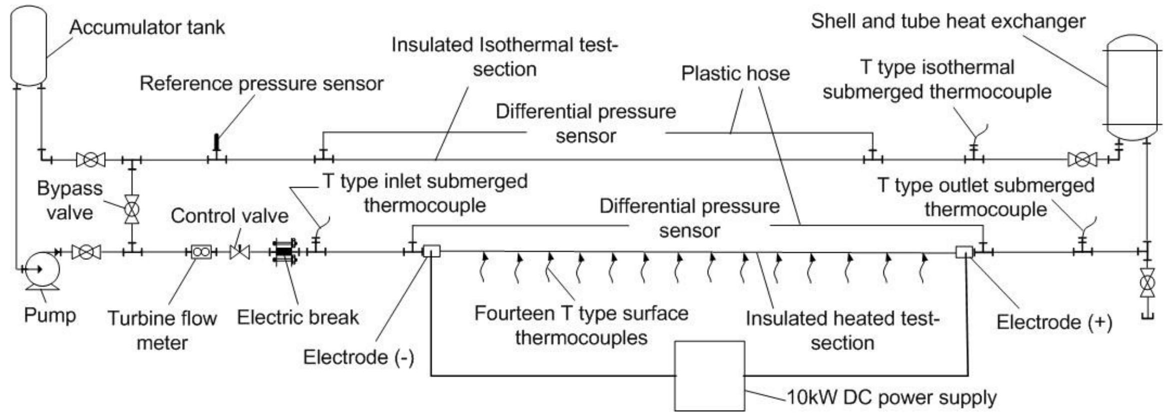

Fig. 1 Diagram of the experimental setup

The turbine flow meter used (FTB-902, OMEGA) was NIST certified with accuracy of 0.5% of the reading. The hot test-fluid was cooled down by means of stainless steel shell-and-tube heat exchanger (35185K52, McMaster-CARR) where the test fluid was in the tube side. In order to measure the pressure drop on both test-sections, OMEGA PX293- 030D5V differential pressure transducers were used. Its operating range is from 0 to 207 kPa (0 to 30 psid) with accuracy to within 0.5% of reading if the reading is greater than 6 psi or 1% if otherwise. A reference gauge pressure sensor (PX302-200GV, OMEGA) with accuracy of 0.25 % BFSL as stated by the manufacturer, was also connected to the loop to have general idea what the pressure inside the loop was.

A stainless steel (SS316) accumulator tank was utilized to charge the loop with the test fluid and also functioned as air vent to ensure that there was no air within the loop. The accumulator tank was exposed to atmospheric pressure. In order to regulate mass flow rate, a flow bypass to the accumulator tank was made available. National Instruments' data acquisition device; i.e., cDAQ-9178, NI 9205, and NI 9213; and LabVIEW 2009 software were chosen to acquire and record all of the data except the voltage and amperage. The data of voltage and amperage of the heated test-section were taken manually by means of, respectively, digital clamp meter and power supply's front panel display. The clamp meter used was KYORITSU KEW SNAP 2055 which has accuracy of 0.5% of reading + 2 digits (0.5% of reading + twice of resolution)

3. Water Convection Heat Transfer

Initial tests were conducted in order to verify the reliability of the experimental facilities for measuring heat transfer coefficient and pressure drop. Water was used in these tests since its performance and properties are well known in literature. The tests were done for Reynolds number ranging from 8,800 to 37,000. The temperature of the heated test-section was maintained to be less than 80 °C to avoid damage of the vinyl electrical tape used to hold the surface thermocouples. The heat transfer coefficient was determined from

$$q'' = h\left(T_{s,i} - T_b\right) \tag{1}$$

Where

$$q'' = \frac{q}{\pi D_i L} = \frac{\dot{m} c_p \left(T_{b,out} - T_{b,in}\right)}{\pi D_i L} \tag{2}$$

The inner surface temperature, Ts,i, was calculated by means of the analytical solution of heat equation with boundary conditions of perfectly insulated tube and known (measured) outer surface temperature, Ts,o.

$$T_{s,i} = T_{s,o} + \frac{\dot{q}}{16k_{ss}}\left({D_o}^2 - {D_i}^2\right) - \frac{\dot{q}}{8k_{ss}}\left({D_o}^2\right) \ln\frac{D_o}{D_i} \tag{3}$$

Where

$$\dot{q} = \frac{\dot{m}c_p\left(T_{b,out} - T_{b,in}\right)}{(1/4)\pi\left({D_o}^2 - {D_i}^2\right)L} \tag{4}$$

and the temperature dependent value of thermal conductivity of SS316, k_{ss}, was calculated by the following polynomial correlation taken from the website of Advanced Energy Tech. Group Center for Energy Research (2011).

$$k_{ss} = 9.0109 + 1.5298 \times 10^{-2} T_{s,o,abs} \quad (5)$$

where $T_{s,o,abs}$ was the outer surface temperature of the stainless steel tube in Kelvin.

Except for the inlet and outlet, the local bulk temperatures were calculated using conservation of energy

$$T_{b-x} = \frac{q"\pi D_i x}{\dot{m} c_p} + T_{b,in} \quad (6)$$

Once local bulk temperature, T_{b-x}, and local inner surface temperature, $T_{s,i-x}$, were known, the local heat transfer coefficient, h_x, was obtained from Eq. (1). Afterwards, this value of heat transfer coefficient was compared to that calculated by Gnielinski's correlation shown by Eq. (7). For simplicity of presentation, the subsequent analysis was based on the average heat transfer coefficient, h_{ave}, along the tube/test-section. The local heat transfer coefficient was used only to verify that the setup was able to produce reliable data.

$$Nu_x = \frac{h_x D_i}{k_x} = \frac{(f_x/8)(Re_x - 1000)Pr_x}{1 + 12.7(f_x/8)^{1/2}(Pr_x{}^{2/3} - 1)} \quad (7)$$

4. Water Pressure Drop Measurement

The measured pressure drop, ΔP, was compared to that obtained from conventional pressure drop theory as follows

$$\Delta P = f(L/D_i)(\rho v^2/2) \quad (8)$$

where the friction factor, f, was:

$$f = 0.316 Re^{-0.25} \quad (9)$$

when Re < 30000 (Blausius relation) or otherwise ($Re \geq 30000$) was based on McAdams relation

$$f = 0.184 Re^{-0.2} \quad (10)$$

Both of these smooth tube turbulent flow relations are actually approximation of Colebrook's formula of friction factor which is accurate to 10 - 15%.

5. The Nanofluid

5.1. Nanofluid properties

The dilute and stable DI water-based CuO nanofluid (CuO-water) used were manufactured and characterized by DR. Abdulaziz Bagabas' research group at National Nanotechnology Center (NNC), King Abdulaziz City for Science and Technology (KACST). The concentration, $\emptyset$, was measured by means of Inductively Coupled Plasma (ICP) and found to be 0.01 vol.%. Its particles have almost spherical shape with diameter range around 5-50 nm as shown in Transmission Electron Microscope (TEM) photos (Fig. 2).

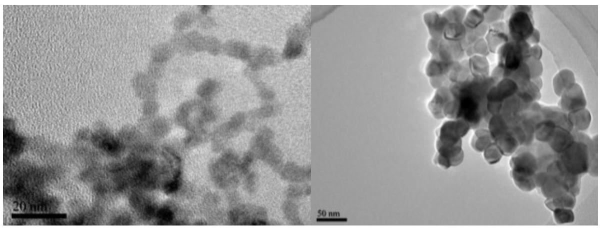

Fig. 2 TEM photos showing the shape and diameter of the CuO nanoparticles

The average particle diameter, 28 nm, was taken based on the average of the maximum and minimum particle size shown by TEM due to lack of information about the particle size distribution. However, the six TEM pictures taken (four of them are not shown here) showed that this diameter estimation is reasonable.

The viscosity of the nanofluid was estimated using Einstein's equation which is valid for spherical particles and only for particle concentration less than 1 vol.% (Williams 2007).

$$\mu_n = \mu_w(1 + 2.5\emptyset) \quad (11)$$

Yu and Choi's (2003) model was used to estimate its thermal conductivity.

$$k_n = k_w \left(\frac{k_p + 2k_w + 2(k_p - k_w)(1+\beta)^3 \emptyset}{k_p + 2k_w - (k_p - k_w)(1+\beta)^3 \emptyset} \right) \qquad (12)$$

where β is ratio between the nanolayer thickness surrounding the nanoparticle and the nanoparticle radius. Yu and Choi showed that this model matches the thermal conductivity data of CuO-EG nanofluid which has nanoparticle radius of 15 nm if it is assumed that the nanolayer thickness to be 2 nm ($\beta \approx 0.13$). Based on this, in this study, β was set to be 0.1.

The density was calculated based on the nanoparticles' proportion as shown below:

$$\rho_n = \emptyset \rho_p + (1 - \emptyset)\rho_w \qquad (13)$$

The constant pressure specific heat was estimated as follows:

$$c_{p,n} = \left[\emptyset \rho_p c_{p,p} + (1 - \emptyset)\rho_w c_{p,w}\right] / \rho_n \qquad (14)$$

5.2. Nanofluid Heat Transfer and Pressure Drop Behavior

Nanofluid heat transfer coefficient and pressure drop were measured and compared to those predicted by Gnielinski correlation and pressure drop theory in conjunction with the aforementioned nanofluid's properties. This was done to see whether conventional correlations can predict nanofluid's heat transfer and pressure drop since there are still contradiction between researchers regarding this. Next, nanofluid's heat transfer coefficient was compared to that of water to see if dilute nanofluid can outperform water in heat transfer performance with insignificant increase in viscosity, and, hence pressure drop.

6. Experimental Uncertainty

The uncertainty was estimated by using the method documented in The ANSI/ASME International's PTC 19.1 Test Uncertainty (Figliola and Beasley, 2005). Here, the uncertainty was calculated from two types of error, i.e., random error and systematic error.

The bias error, B, was taken from the manufacturer's manual of the device and the random error, P, was estimated by only taking into account the temporal variation of the reading in each experimental run. The equation used to estimate the uncertainty, u, of variables which value was obtained from direct measurement was as follow.

$$u = \sqrt{B^2 + (t_{\nu,95})P^2}$$

where $t_{\nu,95}$ was determined to be equal to two since the number of samples was large (N = 360). This amount of data was taken within 3 minutes of experiment. As for variable which was dependent on other variables, the propagation of uncertainty equation was used.

In the calculation, uncertainties of all variables were taken into account accept for those which were negligible, i.e., the uncertainties of fluid's density, nanoparticle's density, nanofluid's concentration, and nanoparticle's specific heat. It was found that the uncertainties were ranging from 5 - 9%, 5 - 9%, and 2% for h, Nu_{ave}, and f, respectively.

7. Results and Discussion

7.1. Water Tests

The water tests conducted show that the experimental apparatus is reliable to measure the convection heat transfer and pressure drop behavior of turbulent liquid flow. This conclusion is based on the good agreement between the results of water tests (six tests) and the results predicted by Gnielinski's correlation for convection heat transfer coefficient and by pressure drop theory for the pressure drop. Figure 3 shows the comparison of the measured local heat transfer coefficient, h_x, to those predicted by Gnielinski's correlation. In this figure, the local h is calculated based on actual measurements, i.e., the heat loss is put into account using Eq. (2).

Moreover, the local h of water which is calculated by putting into account the heat loss is also compared to that with no heat loss assumption (heat transferred to the fluids equals the product of voltage and current of the test-section) in order to see how the heat loss affects the local h. The results show small discrepancies of less than 5% which verifies that the perfectly insulated tube assumption used to calculate the inner surface temperature, $T_{s,i}$, is valid.

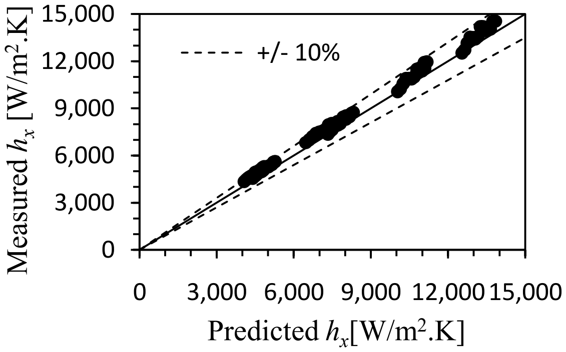

Fig. 3 Comparison between measured and predicted (Gnielinski's corr.) local h of water

Regarding the pressure drop, the measurement results in both, heated and isothermal test section, agreed to the theory to within 10% as expected since the accuracy of the theory itself is between 10 – 15%.

7.2. Nanofluid Tests

7.2.1. Comparison to conventional correlation

Six tests have been conducted for 0.01 vol.% CuO-water nanofluids and the measured average heat transfer coefficient is compared to that predicted by Gnielinski's correlation in conjunction with the nanofluid's properties for obtaining the dimensionless numbers (*Re, Pr,* and *f*). It is found that the heat transfer coefficient agrees well to within 10% with that predicted (Fig. 4). Hence, for this particular nanofluid, it can be concluded that conventional correlation such as Gnielinki's correlation still can be used to predict its heat transfer behavior. The same happens also to the pressure drop results, i.e., the theory can well predict the measured pressure drop (Fig. 5 and 6)

7.2.2. Comparison with water

Here, the heat transfer coefficient of water will be compared to that of the nanofluid considered. It is preferred to compare these fluids based on a number combining *Re* and *Pr* because the dimensionless general heat equation that governs the temperature profile and, therefore, the temperature gradient at surface are function of *Re* and *Pr*. It is known that the temperature gradient at surface determines the heat transfer coefficient. Furthermore, the combination of *Re* and *Pr* chosen is $Re^{0.8}Pr^{0.4}$ which is inspired by Dittus-Boelter correlation.

Figure 7 shows that the Nusselt number of the nanofluid are 0.8% higher than that of the water at the same $Re^{0.8}Pr^{0.4}$ number. The calculation of this 0.8%-difference is based on linear fit value of water results and of nanofluid results. This finding shows that this very dilute CuO nanofluid does not give significant increase in the heat transfer performance compared to that of water since it is still within the uncertainty range of the experimental results, i.e., 5-9% for Nu_{ave}. Thus, it indicates that the dispersed nanoparticles do not show any abnormal behavior which causes an abnormal increase in heat transfer. This also means that it is merely the matter of change in its thermophysical properties. As estimated by Eq. (11) and Eq. (12), the μ and k of this nanofluid are nearly the same as those of water where the increase are only, respectively, 0.025% and no more than 0.04% and therefore, it is not surprising for both fluids to have similar heat transfer performance. However, a higher concentration of CuO-water nanofluids must be tested to find the possibilities of a concentration-threshold for which the nanoparticle chaotic movement, Brownian motion and nanoparticle migration affect the heat transfer as had been pointed out by Heris et al. (2007).

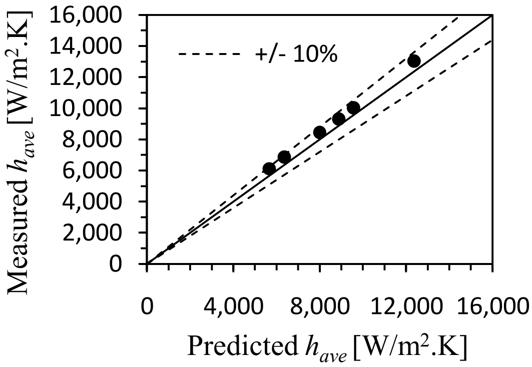

Fig. 4 Comparison between measured and predicted average h of CuO-water, 0.01 vol.%

The pressure drop of the nanofluids and water will be presented in terms of friction factor, *f*, as a function of $Re^{-0.25}$ which is taken based on Blausius correlation. The results of both fluids show that their friction factor and hence, their pressure drop, are comparable (Fig. 8). This result is expected since the properties of the nanofluids, especially the viscosity in this regard, are similar to that of water, i.e., only 0.025% higher.

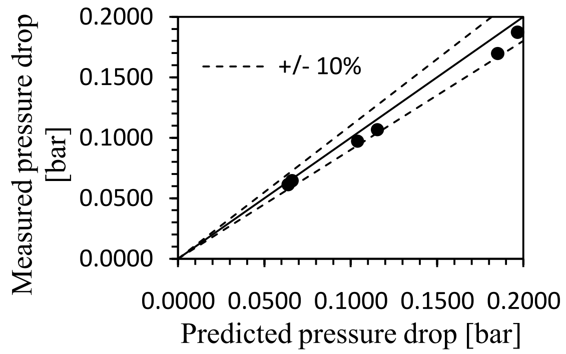

Fig. 5 Pressure drop comparison of CuO-water, 0.01 vol.% at the heated test-section

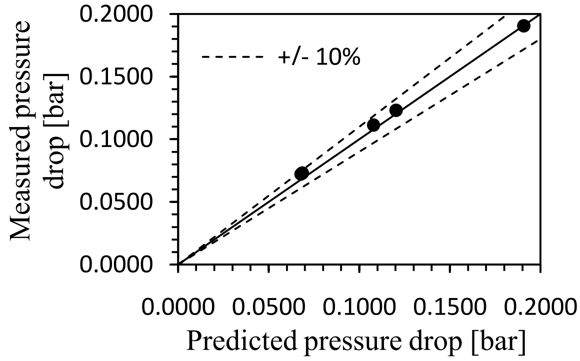

Fig. 6 Pressure drop comparison of CuO-water, 0.01 vol.% at the isothermal test-section

8. Conclusions

Experiment on turbulent (Re of 11,500 to 32,000) forced convective heat transfer and pressure drop of 0.01 vol.% CuO-water nanofluid within circular tube under constant uniform heat flux condition has been conducted and it can be concluded as follows:

1. Traditional correlation such as Gnielinski's correlation; in conjunction with the nanofluid's properties to calculate the dimensionless parameter; can predict the heat transfer of the nanofluid considered.
2. This finding shows that this very dilute CuO nanofluid does not give significant increase in the heat transfer performance compared to that of water. Thus, it indicates that the dispersed nanoparticles do not show any abnormal behavior which causes an abnormal increase in heat transfer. This also means that it is merely the matter of change in the nanofluid's thermophysical properties.

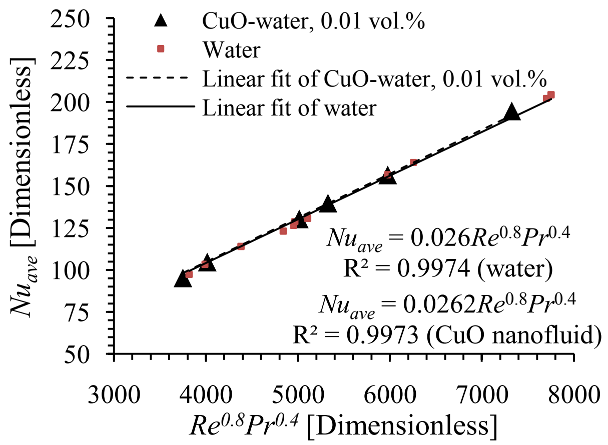

Fig. 7 Experimental Nusselt number at different $Re^{0.8}Pr^{0.4}$

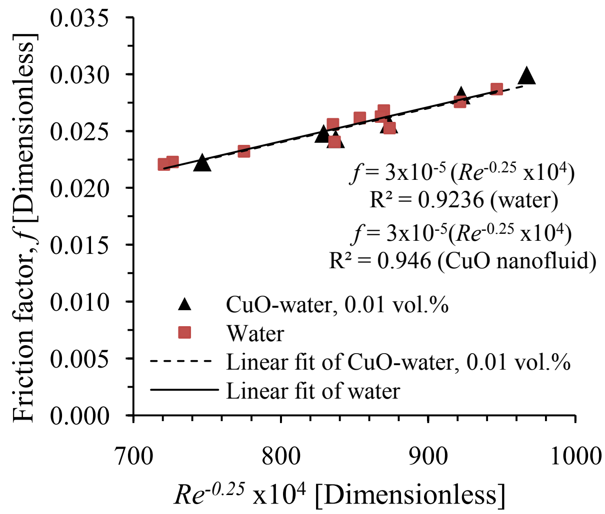

Fig. 8 Measured friction factor at different $Re^{-0.25}$ x10^4 in the heated section

3. The pressure drop of the nanofluid can be predicted by conventional pressure drop theory in conjunction with nanofluid's properties to obtain the dimensionless parameters. Moreover, as expected, the pressure drop is almost the same as that of water since the difference in thermophysical properties between them is small. Thus, there is no anomaly in pressure drop of the nanofluid due to the dispersed nanoparticles.

Acknowledgment

This research is fully supported by KACST (King Abdulaziz City for Science and Technology). Special thanks are conveyed to DR. Khalid al-

Dakkan from KACST as the manager of this nanofluids research project.

Nomenclature

c_p	Specific heat at constant pressure	J/kg K
d	Particle diameter	nm
D	Tube diameter	m
DI	Deionized	Dimensionless
EG	Ethylene glycol	Dimensionless
f	Friction factor	Dimensionless
h	Heat transfer coefficient	W/m^2 K
k	Thermal conductivity	W/m K
L	Tube length	m
$\dot{m}$	Mass flow rate	kg/s
Nu	Nusselt number	Dimensionless
Pe	Peclet number	Dimensionless
Pr	Prandtl number	Dimensionless
q''	Heat flux	W/m^2
$\dot{q}$	Volumetric heat generation	W/m^3
Re	Reynolds number	Dimensionless
T	Temperature	^oC
T_{abs}	Absolute temperature	K
v	Mean velocity	m/s
x	Distance from the beginning of the heated section	m
Greek		
ϕ	Nanoparticle vol. fraction	Dimensionless
μ	Viscosity	Pa s
ρ	Density	kg/m^3
ΔP	Pressure drop	Pa

Subscript

ave	Average
b	Bulk
i	Inner
in	Inlet
n	Nanofluid
o	Outer
out	Outlet
p	Nanoparticle
s	Surface
ss	Stainless steel
w	Water
x	At location *x*

References

Beck, M.P., Sun, T., Teja, A.S., 2007. The Thermal Conductivity of Alumina Nanoparticles Dispersed in Ethylene Glycol. Fluid Phase Equilibria 260, pp. 275-278.

Eastman, J.A., Choi, S.U.S., Li, S., Yu, W., Thompson, L.J., 2001. Anomalously Increased Effective Thermal Conductivities of Ethylene-Glycol-Based Nanofluids Containing Copper Nanoparticles. Appl. Phys. Lett. 78 (6), pp. 718-720.

Figliola, R.S., Beasley, D.E., 2005. Theory and Design for Mechanical Measurements. Wiley, 4th edition, p. 148-182.

Heris, S.Z., Esfahany, M.N., Etemad, S.G., 2007. Experimental Investigation of Convective Heat Transfer of Al_2O_3/water Nanofluids in Circular Tube. Int. J. of Heat and Fluid Flow 28, pp. 203-210.

http://www-ferp.ucsd.edu/LIB/PROPS/PANOS/ss.html, May 20, 2011.

Maiga, S.E.B., Nguyen, C.T., Galanis, N., Roy, G., 2004. Heat Transfer Behaviours of Nanofluids in a Uniformly Heated Tube. Superlattices and Microstructures 35, pp. 543-557.

Murshed, S.M.S., Leong, K.C., Yang, C., 2005. Enhanced thermal conductivity of TiO_2-water based nanofluids. Int. J. of Thermal Sciences 44, pp. 367-373.

Williams, W.C., 2007. Experimental and Theoretical Investigation of Transport Phenomena in Nanoparticle Colloids (Nanofluids). Ph.D. thesis, Massachusetts Institute of Technology, Cambridge, Massachusetts.

Williams, W.C., Buongiorno, J., Hu, L.W., 2008. Experimental Investigation of Turbulent Convective Heat Transfer and Pressure Loss of Alumina/Water and Zirconia/Water Nanoparticle Colloids (Nanofluids) in Horizontal Tubes. ASME J. Heat Transfer 130(4), 7 pages.

Xuan, Y., Li, Q., 2003. Investigation on Convective Heat Transfer and Flow Features of Nanofluids. ASME J. Heat Transfer 125(1), pp. 151-155.

Yu, W., Choi, S.U.S., 2003. The role of interfacial layers in the enhanced thermal conductivity of nanofluids: A renovated Maxwell model. Journal of Nanoparticle Research 5, pp. 167–171.

Zhang, X., Gu, H., Fujii, M., 2006. Experimental Study on the Effective Thermal Conductivity and Thermal Diffusivity of Nanofluids. International Journal of Thermophysics 27, pp. 569-580.